### Research Article

Idorenyin Iwe and Zhigang Li\*

# An isothermal, non-enzymatic, and dualamplified fluorescent sensor for highly sensitive DNA detection

https://doi.org/10.1515/revac-2021-0140 received May 04, 2021; accepted August 02, 2021

Abstract: Sensitive DNA assays are of importance in life science and biomedical engineering, but they are heavily dependent on thermal cycling programs or enzymeassisted schemes, which require the utilization of bulky devices and costly reagents. To circumvent such requirements, we developed an isothermal enzyme-free DNA sensing method with dual-stage signal amplification ability based on the coupling use of catalytic hairpin assembly (CHA) and Mg<sup>2+</sup>-dependent deoxyribozyme (DNAzyme). In this study, the sensing system involves a set of hairpin DNA probes for CHA (ensuring the first stage of signal amplification) as well as ribonucleobase-modified molecular beacons that serve as activatable substrates for DNAzymes (warranting the second stage of signal amplification). An experimentally determined detection limit of about 0.5 pM is achieved with a good linear range from 0.5 to 10 pM. The results from spiked fetal bovine serum samples further confirm the reliability for practical applications. The non-thermal cycling, enzyme-free, and dualamplified features make it a powerful sensing tool for effective nucleic acid assay in a variety of biomedical applications.

Keywords: enzyme-free, isothermal, dual-stage signal amplification, catalytic hairpin assembly, DNAzyme

Idorenyin Iwe: Department of Mechanical and Aerospace Engineering, The Hong Kong University of Science and Technology, Clear Water Bay, Kowloon, Hong Kong, China

# 1 Introduction

The sensitive determination of DNA has a crucial role in the diagnosis of infectious diseases, prevention of pandemics, food control, epigenetics, and even forensic investigations [1,2]. Toward this goal, many sensitive methods have been developed, among which the polymerase chain reaction-based methods are widely used due to their remarkable amplification efficiencies. Nevertheless, they have some drawbacks, such as the requirement of costly and precise thermal cycling instruments as well as well-trained staff. Moreover, there can be false results due to the presence of contaminants or inhibitors. To circumvent such challenges, isothermal nucleic acid amplification approaches emerge as promising alternatives. Such isothermal strategies include helicase-dependent amplification (HDA) [3], rolling circle amplification (RCA) [4], and loop-mediated isothermal amplification (LAMP) [5], and so forth [6]. Despite their outstanding amplification performance, they still have limitations that may impede their applications in molecular detections. For example, the reagents used in HDA-based schemes are quite expensive. Moreover, the fabrication of circular templates used in RCA-based sensing systems requires tedious steps. Besides, four or six primers are required in LAMP-based approaches and their design is rather complicated.

Recently, there have been other nucleic acid amplification and quantification methods to address the aforementioned challenges [7-12]. In this regard, there is a strong need to develop simple, cost-effective, and enzymefree nucleic acid amplification strategies for nucleic acid analysis. Catalytic hairpin assembly (CHA) [13,14] and hybridization chain reaction (HCR) [15,16] are two robust enzymefree signal enhancement schemes that are widely used to improve the detection sensitivity in nucleic acid testing [17]. Our group used to develop CHA-based methods via the use of label-free probes [18] and dually tagged probes (molecular beacons [MBs]) [14]. Moreover, Huang et al. also reported an

<sup>\*</sup> Corresponding author: Zhigang Li, Department of Mechanical and Aerospace Engineering, The Hong Kong University of Science and Technology, Clear Water Bay, Kowloon, Hong Kong, China, e-mail: mezli@ust.hk

<sup>👸</sup> Open Access. © 2021 Idorenyin Iwe and Zhigang Li, published by De Gruyter. 😥 💌 This work is licensed under the Creative Commons Attribution 4.0 International License.

HCR-based method for the amplified determination of the DNA target with  $MoS_2$  nanosheets acting as fluorescence quenchers [16]. Despite their system simplicity, purely CHA or HCR-based methods are still not sufficiently effective to detect trace amounts of analytes. Therefore, cascade amplification systems via the collaborative utilization of multiple signal enhancement elements are often deployed to overcome this deficiency [19]. Methods to integrate multiple enzyme-free DNA amplification reactions to further improve the detection performance are still sought after.

Deoxyribozyme or catalytic DNA (DNAzyme) has been identified as a potential biocatalyst for signal generation and amplification [20,21]. It is important to note that DNAzyme techniques are very popular for detecting metal ions [22–24], ATPs [25,26], and so on [27–30]. But it has recently gained increasing research attention in biosensor construction for nucleic acid detection [31–34]. DNAzyme usually comprises single-stranded DNA with a unique sequence, possessing high catalytic ability toward specific substrates [35]. Contrary to protein enzymes, DNAzyme does not rely on any proteins to perform any catalytic function, but can effectively catalyze biochemical reactions using specific metal ion cofactors [36] at low production cost with high resistance to hydrolysis and good stability [37]. Among all the divalent metal ion cofactor-

dependent DNAzymes, Mg<sup>2+</sup>-dependent DNAzymes are widely used in biosensing because of their robust activities and small catalytic cores [36], in addition to their unprecedented ability to circularly cleave ribonucleobase (rA) inserted into the chimeric DNA substrate strands for releasing accumulated signal [38]. The operation of Mg<sup>2+</sup>-dependent DNAzyme is very flexible and can be combined with other amplification methods to further build ultrasensitive detection systems [24]. To date, many DNAzyme systems [39–42] have outperformed some enzyme-free (non-DNAzyme) [2,14–16] and enzyme-assisted [13,43,44] systems with up to three orders of magnitude performance enhancement.

Herein, we present a simple and robust isothermal sensing method for the detection of target DNA with a dual-stage amplification capability, which is realized by the coupling use of both CHA and Mg<sup>2+</sup>-dependent DNAzyme. The sensing system contains a functional set of hairpin DNA probes (HP1 and HP2) as well as a smartly designed MB. The formation of intact DNAzymes is achieved by a regular CHA reaction between HP1 and HP2, which contain two distinct split fragments of DNAzyme. MBs are then continuously cleaved by DNAzymes, and a remarkably amplified fluorescence signal is generated to report the presence of target DNA at low concentrations. It is noted that the target regeneration in the CHA process ensures the first

Table 1: A comparison between the present method and other schemes via the coupling use of DNAzyme and CHA

Enhancement element	Signal measurement	Target	Limit of detection (LOD)	References
DNAzyme + CHA	Fluorescence	Na <sup>+</sup>	14.0 μΜ	[22]
	Fluorescence	Pb <sup>2+</sup>	246.0 pM	[23]
	Fluorescence	Pb <sup>2+</sup>	170.0 pM	[50]
	Electrochemistry	Pb <sup>2+</sup>	95.0 pM	[51]
	Fluorescence	${\sf Hg}^{2+}$	4.5 pM	[24]
	Absorbance	$U0_{2}^{2+}$	0.1 pM	[52]
	Electrochemistry	ATP	0.6 nM	[25]
	Electrochemistry	ATP	0.5 pM	[26]
	Electrochemistry	Ampicillin	1.0 pM	[27]
	Absorbance	Thrombin	1.0 pM	[28]
	Fluorescence	Thrombin	23.0 fM	[53]
	Absorbance	Telomerase	_	[54]
	Fluorescence	Telomerase	_	[29]
	Absorbance	HCV core protein	$0.1\mathrm{fg}\cdot\mathrm{mL}^{-1}$	[30]
	Absorbance	miRNA	0.2 pM	[31]
	Fluorescence	miRNA	15.6 pM	[32]
	Fluorescence	miRNA	1.0 pM	[55]
	Fluorescence	miRNA	37.0 fM	[56]
	Fluorescence	miRNA	6.8 fM	[57]
	Electrochemistry	miRNA	0.5 fM	[58]
	Absorbance	DNA	10.0 aM	[33]
	Fluorescence	DNA	1.0 pM	[33]
	Photoelectrochemistry	DNA	1.2 fM	[34]
	Fluorescence	DNA	0.5 pM	This study

layer of signal amplification, while the catalysis performed by DNAzymes with multiple turnovers is responsible for the second layer of signal enhancement. Moreover, the introduction of self-quenched MBs further helps to suppress the background signal and improve detection selectivity. The specificity and sensitivity of this method have been evaluated both in standard buffer and in serums with a satisfactory outcome at the sub-picomolar level. Table 1 compares the proposed strategy with the recently reported DNAzymeand CHA-mediated systems. Herein, the sensing system is very simple and devoid of protein enzymes and advanced materials with overall performance outweighing many previously reported fluorescence assays [18,45-47]. Considering the superb sensitivity and selectivity, together with the wash-free convenience, mix-and-measure manner, enzyme-free nature, and isothermal features, this coupling CHA and DNAzyme-aided strategy holds great potential for effective nucleic acid assay in a variety of biomedical applications.

# 2 Experimental section

#### 2.1 Chemicals and materials

 $1\times$  PBS buffer (pH = 7.4) was purchased from Gibco Life Technologies (New York, United States, https://www.thermofisher.com), while MgCl<sub>2</sub> was ordered from Sigma-Aldrich Co. (China, www.sigmaaldrich.com). The MBs, hairpin probes (HP1 and HP2), target DNA (T), DNAzyme, and mismatched targets (M1, M3, and M8) were synthesized by Takara Bio Inc. (Dalian, China; www.bio-stationhk.net). The MBs were labeled with a fluorophore dye, fluorescein amidite

(FAM), and a fluorescence quencher (dabcyl) at the 5' and 3' ends, respectively. They were purified with high-performance liquid chromatography, while the other oligos were purified with polyacrylamide gel electrophoresis (PAGE). Part of the sequences of HP1 is complementary to the target DNA while the remaining part is complementary to HP2. All the probes used are illustrated in detail in Table 2. The target DNA and mismatched targets are 23 nt in length. Oligos M1, M3, and M8 contain one, three, and eight mismatched base pairs, respectively, as indicated by the underlined letters in Table 2. All samples were prepared using ultra-pure water (resistivity ≥18.2 MΩ·cm) obtained from a Milli-Q water purification system, and the other reagents were of analytical grade and used without further purification or modification. Each sample was of 200 µL and Mg<sup>2+</sup> was kept at 10 mM for all the experiments. All the experiments were conducted at 24°C.

The PAGE experiments were performed using an electrophoresis analyzer and images were obtained on a Bio-Rad ChemiDoc XRS system, while the fluorescence measurements were performed using a FlexStation 3 Multi-Mode Microplate Reader.

# 2.2 Detection procedure

The lyophilized DNA was dissolved in ultra-pure water to obtain a stock solution of  $100 \,\mu\text{M}$  and stored at  $-20\,^{\circ}\text{C}$ . Before the experiments, the stock solution concentration was further reduced to  $5 \,\mu\text{M}$  using a PBS buffer to serve as working solutions. Thereafter, the solution consisting of HP1, HP2, and MB was annealed separately at  $95\,^{\circ}\text{C}$  in a water bath for  $5 \,\text{min}$  and then allowed to cool

Table 2: Oligonucleotides used in the experiments

Name	Sequence (5'-3')*
Target DNA	CGA CAT CTA ACC TAG CAA GAT CG
M1	CGA CAT CTA <u>T</u> CC TAG CAA GAT CG
M3	CG <u>T</u> CAT CTA <u>T</u> CC TAG CAA G <u>T</u> T CG
M8	CG <u>T</u> C <u>T</u> T CT <u>TT</u> CC T <u>T</u> G C <u>TT</u> G <u>T</u> T CG
HP1	CCGAT ATC AGC GAT CTT GCT AGG TTA GAT GTC GAA GCA CCC ATG TTA CTC TCG ACA TCT AAC CTA GC
HP2	AGA TGT CGA GAG TAA CAT GGG TGC TTC GAC ATC TAA CCT AGC AAG CAC CCA TGT TAC TCT CGA
MB	(FAM)-G CGG GAT GGG AAT TTC GAG AGT ATrA GGA TAT CGG CGT GGG TTC CCG C-(DABCYL)
DNAzyme	CCGAT ATC AGC GAT TAACGCTTATTTTAAGCGTTA CAC CCA TGTTAC TCT CGA

<sup>\*</sup>The underlined bases are the mismatched sequences.

<sup>\*\*</sup>The purple color in HP1, DNAzyme, and MB indicates a complementary sequence, while the red color in HP2, MB, and DNAzyme also shows a complementary sequence. The blue color in HP1 and HP2 indicates the DNAzyme sequence after hybridization with MB, and the same applies to the DNAzyme strand.

down to room temperature for at least 2 h. For detection experiments, various concentrations of target DNA were mixed with HP1 and HP2 (150 nM each), and subsequently, MB (50 nM) was introduced into the reaction buffer containing  $1 \times PBS$  buffer (pH = 7.4) and 10 mM Mg<sup>2+</sup>. The mixture was placed in a Microplate Reader and kinetically scanned to obtain fluorescence intensities. The detection performance was further validated, including the serum sample analysis whose outcomes are presented under Section 3.

# 2.3 Native gel electrophoresis

The annealed samples of HP1, HP2, and MB along with the target DNA were of  $1\,\mu\text{M}$  for gel electrophoresis. Around  $10\,\mu\text{L}$  of different combinations of the reaction mixtures were incubated at  $24\,^{\circ}\text{C}$  for at least 3 h before being loaded into lanes of 3% agarose gel. The gel was allowed to run at 100 V for 40 min under room temperature in a standard TAE buffer purchased from Thermo-Fisher (https://www.thermofisher.com/order/catalog/product/B49), and thereafter photographed using a Bio-Rad digital imaging system after being stained in a SYBR Gold solution for 20 min.

#### 2.4 Fluorescence measurements

The fluorescence data were obtained by using a FlexStation 3 Multi-Mode Microplate Reader with the temperature fixed at 24°C. According to the fluorescence emission properties of FAM-labeled on MB, the excitation and emission wavelengths were set at 490 and 520 nm, respectively. Flat bottom, TC-treated, 96-well plate (black) obtained from Genetimes ExCell International Holdings Limited (Hong Kong) was used to contain the reaction solution. The maximum fluorescence intensity after 1 h was used for detection analysis.

# 3 Results and discussion

# 3.1 Working mechanism

The CHA-DNAzyme-mediated dual-mode amplification sensing scheme is illustrated in Figure 1. The sensing

system comprises two structurally designed hairpin probes (HP1 and HP2) and an MB. The two hairpin probes are intentionally designed to incorporate two separate subunits of spatially split Mg<sup>2+</sup>-dependent DNAzyme fragments, which are presented in an inactive state, except otherwise triggered and assembled as a functionally integrated DNAzyme. The MB is a chimeric DNA probe that contains an rA and serves as a DNAzyme substrate. The 5' and 3' ends are labeled with a fluorophore (FAM) and quencher (dabcyl), which is termed as a fluorescence resonance energy transfer (FRET) pair. The close proximity of the FRET pair leads to a greatly suppressed background signal, while the separation of the FRET pair results in evident signal recovery. The stem-loop domain of HP1 is complementary with the toehold-stem domain of HP2, but the stable hairpin structure of HP1 and HP2 prevents them from hybridizing with each other and thus preserves the hairpins in a double-stranded hybrid state. Similarly, part of the loop domain sequence of the MB is complementary to a section of the toehold of HP1 and the caged bases in the stem fragment of HP2. Interestingly, in the absence of the target DNA, HP1, HP2, and MB could coexist in the solution assuming highly stable hairpin conformations according to the hairpin design principles [48]. Upon introduction of the target DNA into the solution, the target-triggered CHA reaction is initiated (Cycle 1 in Figure 1), and facilitates the binding of HP2 to HP1 while the target DNA is continuously recycled. Thereafter, the exposed toeholds of HP1 and HP2 form a DNAzyme configuration, and the remaining parts are available to bind with the loop domain of the MB (Cycle 2 in Figure 1). In the presence of Mg<sup>2+</sup> ions, the MB is cyclically cleaved at the rA phosphodiester bond to separate the FAM and dabcyl at the MB strands, generating a strong fluorescence signal. After the cleavage, the HP1-HP2 complex is continuously recycled and becomes available to bind with another MB to continue the reaction cycle. Therefore, the dual cycling reaction process remarkably amplifies the fluorescence intensity and thereby enhances detection sensitivity.

# 3.2 Feasibility testing

In order to validate the feasibility of the sensing system, different samples were first analyzed by comparing the fluorescence signals of various combinations. Figure 2a illustrates the fluorescence emission intensities of various sensing systems without the target DNA (MB; MB + HP1; MB + HP2 + Mg $^{2+}$ ; MB + HP1 + HP2 + Mg $^{2+}$ ), the proposed sensing system

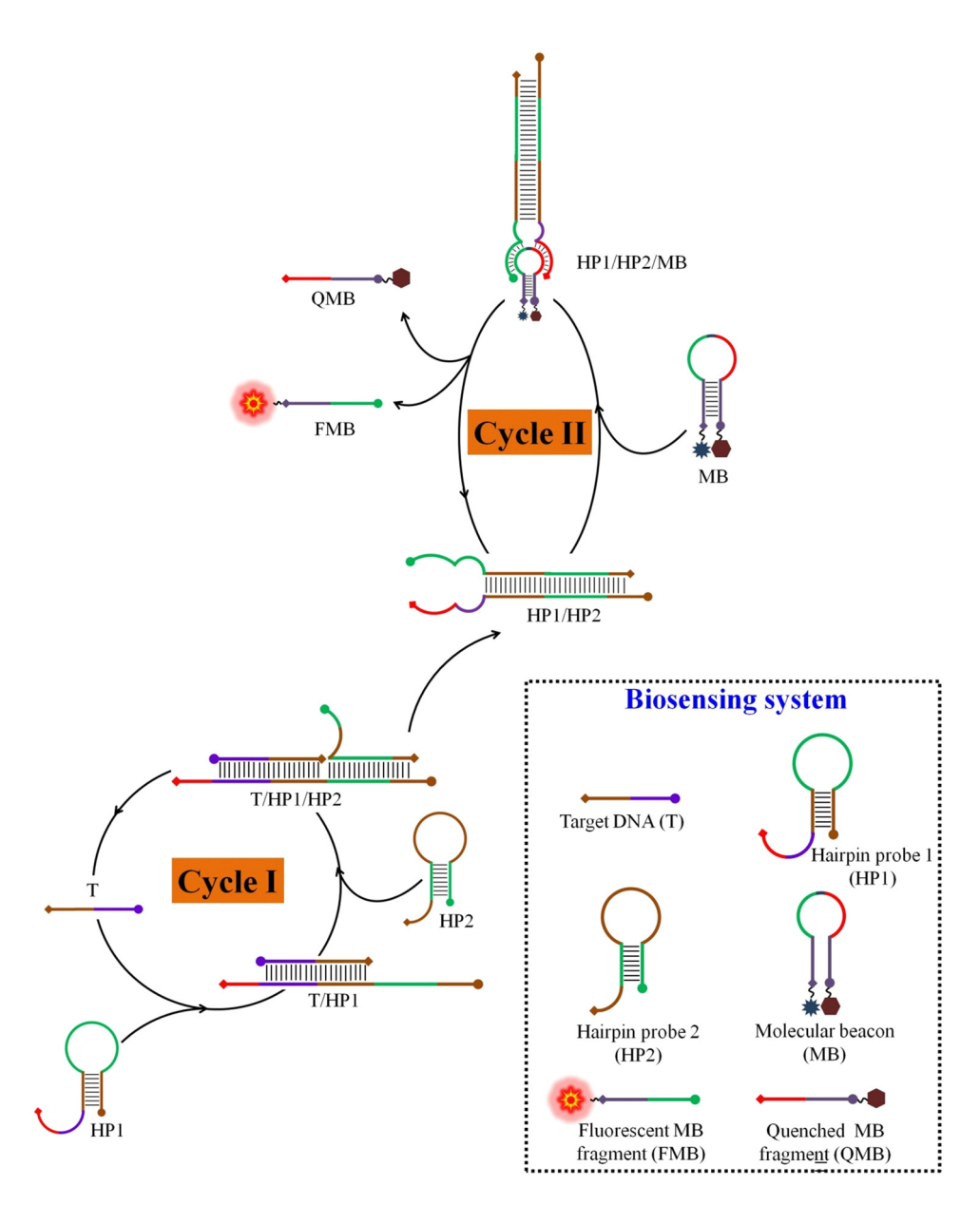
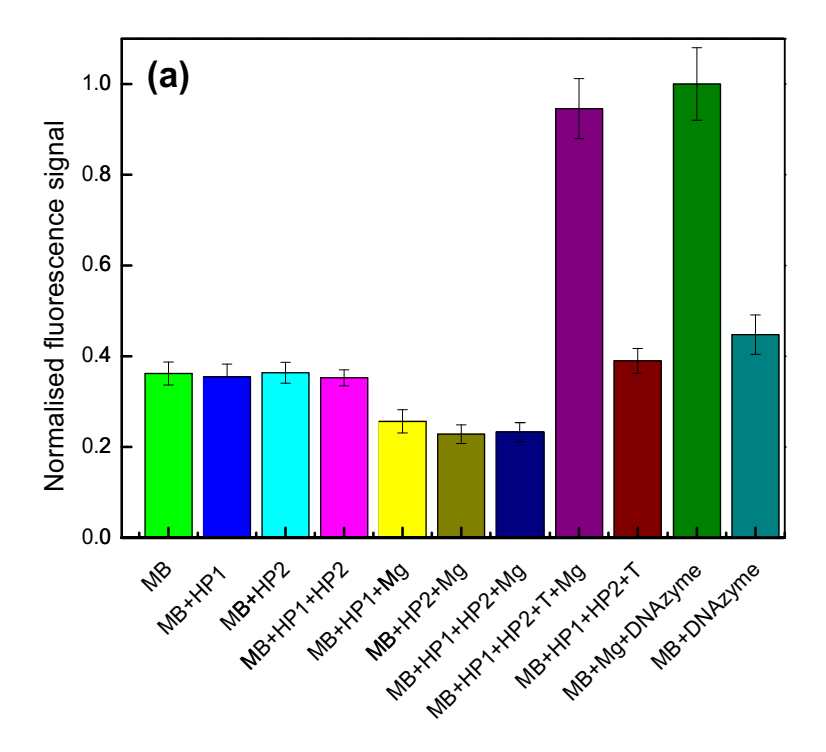


Figure 1: Schematic of the CHA-DNAzyme-assisted dual-mode amplification system for fluorescent detection of target DNA.

(MB + HP1 + HP2 + T + Mg $^{2+}$ ); the proposed sensing system without Mg $^{2+}$  (MB + HP1 + HP2 + T), the traditional DNAzyme system (MB + Mg $^{2+}$  + DNAzyme), and the DNAzyme system without Mg $^{2+}$  (MB + DNAzyme). The samples containing (MB + HP1)/(MB + HP2)/(MB + HP1 + HP2) reported similar response signals as that of the background signal from the sample with only MB involved. However, the signal was further reduced when Mg $^{2+}$  was added into the relevant samples, including samples consisting of (MB + HP1 + Mg $^{2+}$ ), (MB + HP2 + Mg $^{2+}$ ), and (MB + HP1 + HP2 + Mg $^{2+}$ ). This is because the DNA duplexes were further strengthened due to the introduced salt, preventing the undesired occurrence of non-specific hybridization events between

hairpin probes [48]. In the event of the proposed sensing system, a significant signal gain was achieved, indicating that the CHA–DNAzyme system was successfully triggered. To further verify the detection scheme, a DNAzyme strand possessing the same DNA sequences as those of HP1 and HP2 was designed and challenged with the MB (MB + Mg<sup>2+</sup> + DNAzyme). The signal gain was comparable to the proposed sensing system. It is worth noting that the signal ratio of the proposed system with/without Mg<sup>2+</sup> is similar to the signal ratio of the DNAzyme system with/without Mg<sup>2+</sup>, which strongly agrees with the design concept (Figure 2a).

To further validate the formation of CHA and DNAzyme hybrid complexes, PAGE analysis was carried out, whose



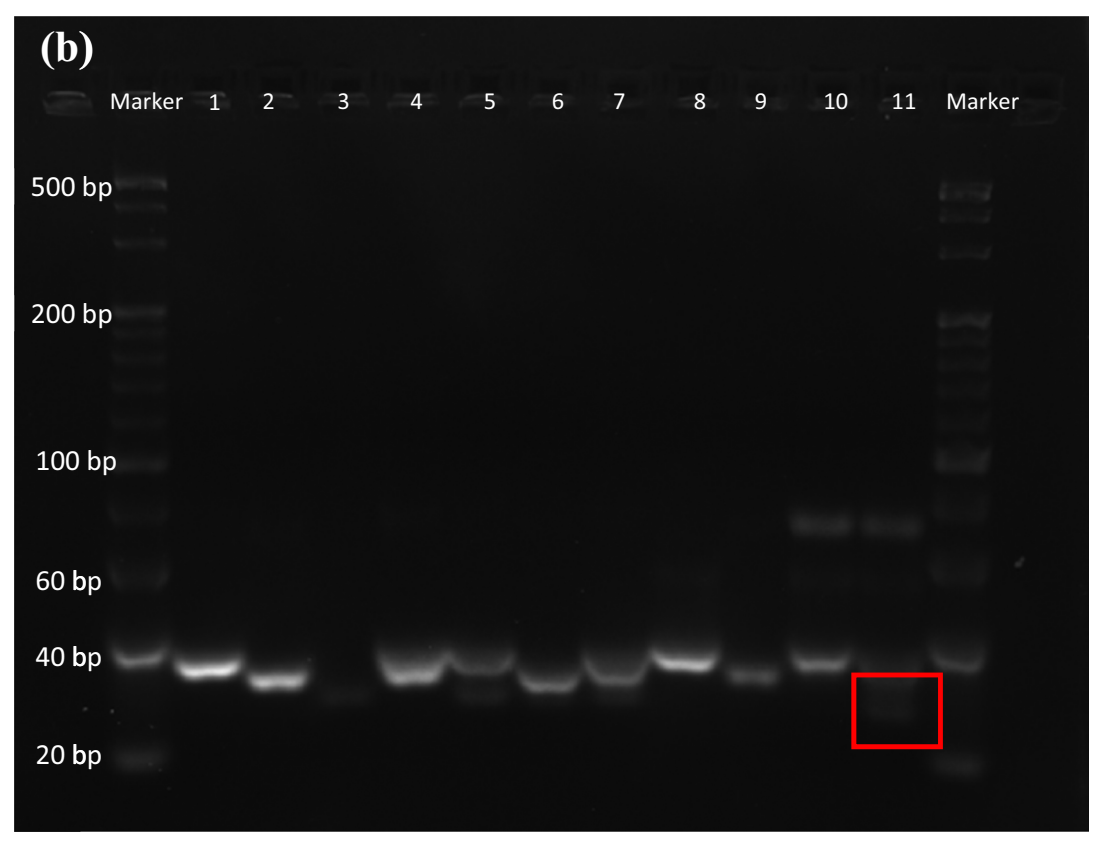
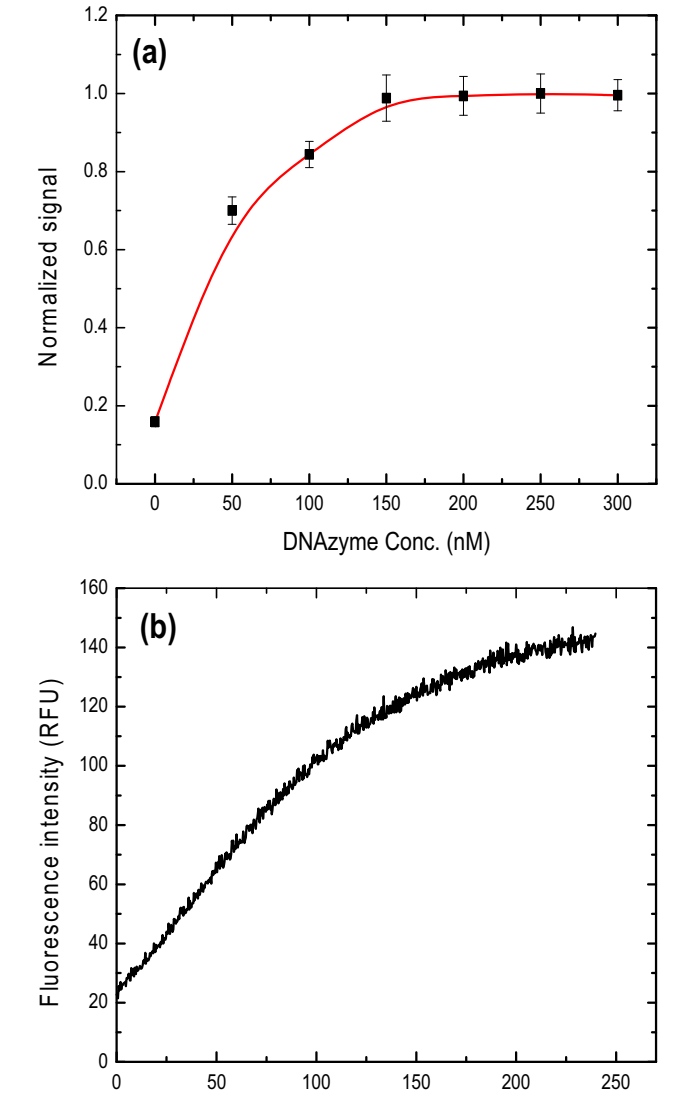


Figure 2: Validation of the detection system. (a) Fluorescence intensities of the sensing system under different conditions. The error bars represent the standard error of three independent measurements. (b) PAGE image of the sensing system. Lane 1: HP1; Lane 2: HP2; Lane 3: MB; Lane 4: HP1 + HP2; Lane 5: MB + HP1; Lane 6: MB + HP2; Lane 7: MB + HP1 + HP2; Lane 8: HP1 + T; Lane 9: HP2 + T; Lane 10: HP1 + HP2 + T; Lane 11: MB + HP1 + HP2 + T. The concentrations of target DNA (T), HP1, HP2, and MB were  $1\mu$ M.

results are detailed in Figure 2b. The mixture samples were in the following sequence: Lane 1: HP1; Lane 2: HP2; Lane 3: MB; Lane 4: HP1 + HP2; Lane 5: MB + HP1; Lane 6: MB + HP2; Lane 7: MB + HP1 + HP2; Lane 8: HP1 + T; Lane 9: HP2 + T; Lane 10: HP1 + HP2 + T; and Lane 11: MB + HP1 + HP2 + T. Lanes 1–3 depict only single species (HP1, HP2, and MB) without self-hybridization, and Lanes 4–7 show a stable coexistence of the mixture of two different species (HP1 + HP2, MB + HP1, and MB + HP2) since there are no visual bands present. In Lane 8, although the introduced target DNA binds with HP1 and forms a 1:1 complex, a visible band could not be observed and the mixture of the target DNA with HP2 in Lane



**Figure 3:** Condition optimization. (a) Normalized signal at various DNAzyme concentrations. The error bars represent the standard error of three independent measurements. (b) Time variation of fluorescence intensity.

Time (min)

9 could not yield any band due to the mismatch between the two species. Lane 10 is a CHA-mediated assay, which is in line with the literature [19], and Lane 11 presents the proposed CHA-DNAzyme-assisted dual-mode amplification scheme with a clear gel band. Compared to Lane 10, the lower band in Lane 11 gradually faded away (red box in Figure 2b) under the influence of the MB, showing faster electrophoretic mobility. This clearly verified the feasibility of the proposed sensing scheme.

# 3.3 Experimental condition optimization

The experimental results are affected by many conditions, and in order to obtain the best analytical performance, the effect of reaction time, HP1, and HP2 was studied in detail, whereas other parameters such as Mg<sup>2+</sup> and MB were fixed based on the previous work of Qi et al. [37] and Iwe et al. [1], respectively.

While studying and changing the parameters of interest, HP1 and HP2 were optimized using the intact DNAzyme strand (sequence in Table 2). Figure 2a clearly shows that the signal ratio of the proposed system with/without Mg<sup>2+</sup> is similar to the signal ratio of the DNAzyme system with/without Mg<sup>2+</sup>, thereby enabling the choice of selecting the DNAzyme strand to further the HP1 and HP2 optimizations. Figure 3a shows the concentration effect of the DNAzyme strand. The fluorescence signal became stable when the DNAzyme concentration reached about 150 nM, which was chosen as the optimized concentration and used to denote the optimum concentration of HP1 and HP2 for the rest of the experiments. The reaction time was monitored in real-time starting from 0 to about 240 min, as presented in Figure 3b. The fluorescence signal began to level off after about 200 min.

# 3.4 Sensitivity investigation

The sensitivity of the sensing system was evaluated under real-time conditions. Figure 4a shows the fluorescence increment in response to different target DNA concentrations within the range of 0–100 nM. In Figure 4a, it is observed that as the target DNA concentrations gradually increased, the corresponding fluorescence intensity also increased. The detection limit was experimentally found to be about 0.5 pM. Figure 4b illustrates the results at 100 min for target DNA concentration from 0 to 100 nM with the inset showing the calibration plot from 0 to 10 pM. The linear fit in the inset gives rise to the theoretical detection limit: 2 pM, which is calculated from three

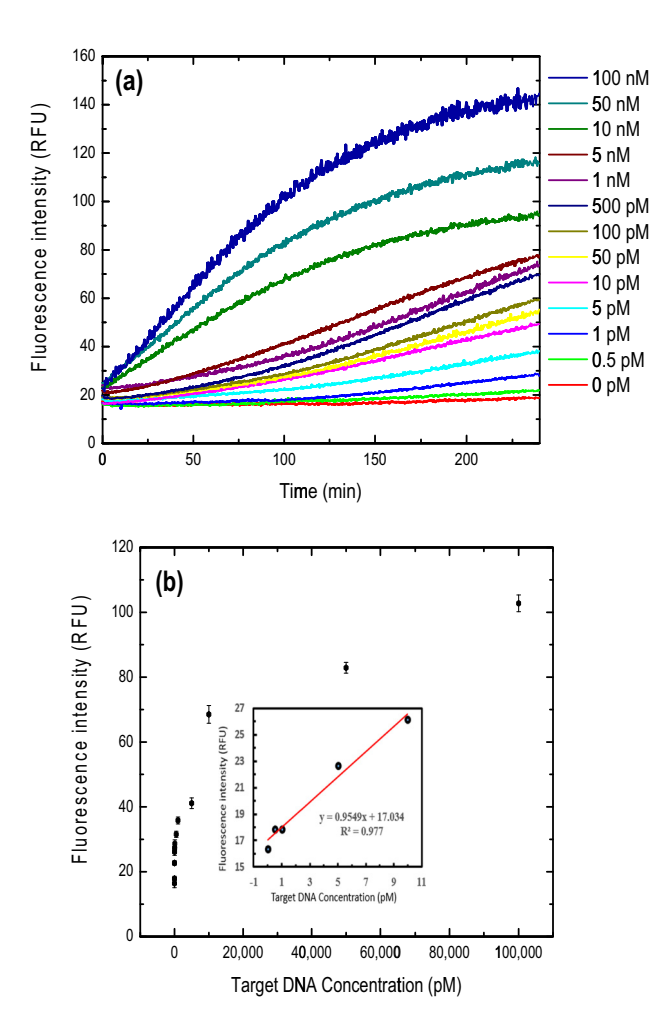


Figure 4: Sensitivity analysis. (a) Fluorescence intensity under various target concentrations. (b) Fluorescence responses after 100 min for different target DNA concentrations. The inset shows a linear relationship at a low concentration regime from 0 to 10 pM. The error bars represent the standard error of three independent measurements.

times the standard deviation of blank fluorescence signal divided by the slope of the regression equation. The sensitivity results have shown significant improvements when compared to the previously reported DNAzyme schemes (reviewed in ref. [36]) due to the coupling effect of CHA. Many enzyme-free [2,14–16] and enzyme-assisted [13,43,44] systems could not also measure up with the performance of the proposed sensing scheme. Table 1 presents a broader comparison of our solution to other past sensing methods.

# 3.5 Specificity examination

Besides the detection sensitivity, specificity is another important factor to evaluate the performance of a sensing

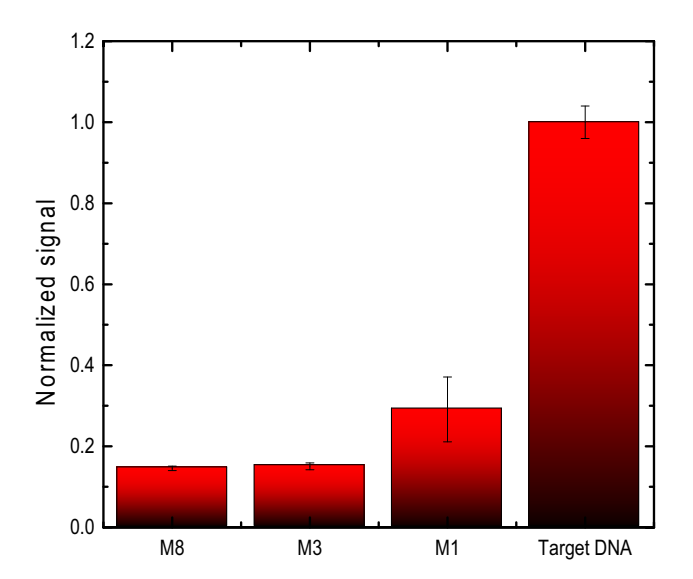


Figure 5: Selectivity examination of the DNAzyme-CHA-based system against different DNA mismatched species. The error bars represent the standard error of three independent measurements.

system. To assess the selectivity of the proposed method, experiments were conducted by using 1, 3, and 8 base-mismatched DNA species designated as M1, M3, and M8, respectively. The response signals at 520 nm emission wavelength were discriminated toward a perfectly matched DNA target (Figure 5). The signal comparison clearly shows that the sensing scheme has a high selectivity against mismatched targets and has the potential to be applied in early-stage disease diagnosis and screening.

# 3.6 Serum sample analysis

To test the practical application of the proposed detection method, further detection was carried out in fetal bovine serum (FBS), which served as a complex biological environment. The FBS was kept at 5% due to the inherent fluctuation of fluorescence signals at increasing concentrations, and the exposure time was kept the same as those with the buffer, to maintain similar experimental conditions. Repetitive and independent measurements were performed with 1, 5, and 10 pM targets, respectively,

Table 3: Target DNA recovery tests with FBS

Sample	Added target (pM)	Found (pM)	Recovery (%)
1	1.0	$0.95\pm0.06$	94.6
2	5.0	$5.98 \pm 0.39$	119.6
3	10.0	$11.59\pm0.93$	115.9

with a recovery rate ranging from 94.6% to 119.6% as presented in Table 3. The results from the FBS indicated that the proposed sensing strategy is capable of analyzing complex biomatrices.

# 4 Conclusion

A CHA-DNAzyme sensing system for target DNA amplification has been proposed. The system takes advantage of the Mg<sup>2+</sup>-dependent DNAzyme methods and CHA techniques and integrates them to develop an isothermal, enzyme-free, robust, and reliable target DNA detection system without incorporating any protein enzymes or precise temperature controllers. The dual-mode amplification strategy enhances the signal gain, thus leading to a highly sensitive system with a detection limit down to 0.5 pM. Compared to enzyme-based methods, the proposed CHA-DNAzyme-enhanced system, which is an enzyme-free detection scheme, has demonstrated significant detection improvement with LOD at 0.5 pM against some enzyme-driven systems with LOD beyond 1 pM [13,44,49]. The detection method is simple, sensitive, and specific compared to the many reported DNAzymeor CHA-assisted strategies. However, the detection time is longer than 1h, which might pose some detection challenges. Other than this, the proposed amplification method is capable of being used to detect different nucleic acid species in complex biomatrices. Therefore, this CHA-DNAzyme may offer insights into the construction of enzyme-free and signal-amplifiable biosensors.

**Funding information:** This work was partially supported by the Research Grants Council of the Hong Kong Special Administrative Region under Grant no. 16209119.

**Author contributions:** Authors contributed equally to this work.

**Conflict of interest:** Authors state no conflict of interest.

# References

- Iwe IA, Li Z, Huang J. A dual-cycling fluorescent scheme for ultrasensitive DNA detection through signal amplification and target regeneration. Analyst. 2019;144:2649-55.
- [2] Huang J, Wang Z, Kim J, Su X, Li Z. Detecting arbitrary DNA mutations using Graphene oxide and Ethidium bromide. Anal Chem. 2015;87:12254–61.

- [3] Ma F, Liu M, Tang B, Zhang C. Sensitive quantification of microRNAs by isothermal helicase-dependent amplification. Anal Chem. 2017;89:6182-7.
- [4] Soares RR, Varela JC, Neogi U, Ciftci S, Ashokkumar M, Pinto IF, et al. Sub-attomole detection of HIV-1 using padlock probes and rolling circle amplification combined with microfluidic affinity chromatography. Biosens Bioelectron. 2020:166:112442.
- [5] Azizi M, Zaferani M, Cheong SH, Abbaspourrad A. Pathogenic bacteria detection using RNA-based loop-mediated isothermal-amplification-assisted nucleic acid amplification via droplet microfluidics. ACS Sen. 2019;4:841–8.
- Zhao Y, Chen F, Li Q, Wang L, Fan C. Isothermal amplification of nucleic acids. Chem Rev. 2015;115:12491–545.
- [7] Papamatthaiou S, Estrela P, Moschou D. Printable graphene BioFETs for DNA quantification in Lab-on-PCB microsystems. Sci Rep. 2021;11:1-9.
- [8] Sui J, Gandotra N, Xie P, Lin Z, Scharfe C, Javanmard M. Multifrequency impedance sensing for detection and sizing of DNA fragments. Sci Rep. 2021;11:1–9.
- [9] Wang M, Guo H, Xue R, Guan Q, Zhang J, Zhang T, et al. A novel electrochemical sensor based on MWCNTs-COOH/metalcovalent organic frameworks (MCOFs)/Co NPs for highly sensitive determination of DNA base. Microchem J. 2021;167:106336.
- [10] Uygun ZO, Atay S. Label-free highly sensitive detection of DNA approximate length and concentration by impedimetric CRISPR-dCas9 based biosensor technology. Bioelectroch. 2021;140:107812.
- [11] Alexaki K, Giust D, Kyriazi M, El-Sagheer AH, Brown T, Muskens OL, et al. DNA sensor based on upconversion nanoparticles and two-dimensional dichalcogenide materials. Front Chem Sci Eng. 2021;15:935–43.
- [12] Cheng Y, Kargupta R, Ghoshal D, Li Z, Chande C, Feng L, et al. ESSENCE-A rapid, shear-enhanced, flow-through, capacitive electrochemical platform for rapid detection of biomolecules. Biosens Bioelectron. 2021;182:113163.
- [13] Iwe IA, Li Z, Huang J. Graphene oxide and enzyme-assisted dual-cycling amplification method for sensitive fluorometric determination of DNA. Microchim Acta. 2019;186:716.
- [14] Huang J, Su X, Li Z. Enzyme-free and amplified fluorescence DNA detection using bimolecular beacons. Anal Chem. 2012;84:5939–43.
- [15] Huang J, Gao X, Jia J, Kim J, Li Z. Graphene oxide-based amplified fluorescent biosensor for Hg2 detection through hybridization chain reactions. Anal Chem. 2014;86:3209-15.
- [16] Huang J, Ye L, Gao X, Li H, Xu J, Li Z. Molybdenum disulfidebased amplified fluorescence DNA detection using hybridization chain reactions. J Mater Chem B. 2015;3:2395–401.
- [17] Iwe IA, Li W, Li Z, Huang J. Hairpin DNA-mediated isothermal amplification (HDMIA) techniques for nucleic acid testing. Talanta. 2021;226:122146.
- [18] Huang J, Su X, Li Z. Enzyme-and label-free amplified fluorescence DNA detection using hairpin probes and SYBR Green I. Sens Actuat B Chem. 2014;200:117–22.
- [19] Quan K, Huang J, Yang X, Yang Y, Ying L, Wang H, et al. Powerful amplification cascades of FRET-based two-layer nonenzymatic nucleic acid circuits. Anal Chem. 2016;88:5857-64.

- [20] Zhu L, Li G, Shao X, Huang K, Luo Y, Xu W. A colorimetric zinc(II) assay based on the use of hairpin DNAzyme recycling and a hemin/G-quadruplex lighted DNA nanoladder. Microchim Acta. 2020;187:26.
- [21] Zheng L, Qi P, Zhang D. DNA-templated fluorescent silver nanoclusters for sensitive detection of pathogenic bacteria based on MNP-DNAzyme-AChE complex. Sens Actuat B Chem. 2018:276:42-7.
- [22] Wu Z, Fan H, Satyavolu NSR, Wang W, Lake R, Jiang J, et al. Imaging endogenous metal ions in living cells using a DNAzyme-catalytic hairpin assembly probe. Angew Chem. 2017;129:8847-51.
- [23] Wu M, Wang G, Chu LT, Huang H, Chen T. Cascade-amplified microfluidic particle accumulation enabling quantification of lead ions through visual inspection. Sens Actuat B Chem. 2020;324:128727.
- [24] Li X, Xie J, Jiang B, Yuan R, Xiang Y. Metallo-toehold-activated catalytic hairpin assembly formation of three-way DNAzyme junctions for amplified fluorescent detection of Hg2. ACS Appl Mater Interf. 2017;9:5733-8.
- [25] Li X, Yang J, Xie J, Jiang B, Yuan R, Xiang Y. Cascaded signal amplification via target-triggered formation of aptazyme for sensitive electrochemical detection of ATP. Biosens Bioelectron. 2018;102:296-300.
- [26] Xie H, Chai Y, Yuan Y, Yuan R. Highly effective molecule converting strategy based on enzyme-free dual recycling amplification for ultrasensitive electrochemical detection of ATP. Chem Commun. 2017;53:8368-71.
- [27] Zhang R, Li S, Wang J, Qu X, Zhao Y, Liu S, et al. Entropy-driven spliced DNA walking machine for label-free electrochemical detection of antibiotics. Sens Actuat B Chem. 2020;320:128385.
- [28] Yin C, Jiang D, Xiao D, Zhou C. An enzyme-free and label-free visual sensing strategy for the detection of thrombin using a plasmonic nanoplatform. Analyst. 2020;145:2219-25.
- [29] Fan H, Bai H, Liu Q, Xing H, Zhang X, Tan W. Monitoring telomerase activity in living cells with high sensitivity using cascade amplification reaction-based nanoprobe. Anal Chem. 2019;91:13143-51.
- [30] Li X, Yin C, Wu Y, Zhang Z, Jiang D, Xiao D, et al. Plasmonic nanoplatform for point-of-care testing trace HCV core protein. Biosens Bioelectron. 2020;147:111488.
- [31] Zhang D, Wu C, Luan C, Gao P, Wang H, Chi J, et al. Distancebased quantification of miRNA-21 by the coffee-ring effect using paper devices. Microchim Acta. 2020;187:1-7.
- [32] Zou L, Wu Q, Zhou Y, Gong X, Liu X, Wang F. A DNAzymepowered cross-catalytic circuit for amplified intracellular imaging. Chem Commun. 2019;55:6519-22.
- [33] Yin C, Wu Y, Li X, Niu J, Lei J, Ding X, et al. Highly selective, naked-eye, and trace discrimination between perfect-match and mismatch sequences using a plasmonic nanoplatform. Anal Chem. 2018;90:7371-6.
- [34] Fan J, Zang Y, Jiang J, Lei J, Xue H. Beta-cyclodextrin-functionalized CdS nanorods as building modules for ultrasensitive photoelectrochemical bioassay of HIV DNA. Biosens Bioelectron. 2019;142:111557.
- [35] Orbach R, Mostinski L, Wang F, Willner I. Nucleic acid driven DNA machineries synthesizing Mg<sup>2</sup>-dependent DNAzymes: an interplay between DNA sensing and logic-gate operations. Chem A Eur J. 2012;18:14689-94.

- [36] Peng H, Newbigging AM, Wang Z, Tao J, Deng W, Le XC, et al. DNAzyme-mediated assays for amplified detection of nucleic acids and proteins. Anal Chem. 2018;90:190-207.
- [37] Qi L, Zhao Y, Yuan H, Bai K, Zhao Y, Chen F, et al. Amplified fluorescence detection of mercury(II) ions (Hg2) using targetinduced DNAzyme cascade with catalytic and molecular beacons. Analyst. 2012;137:2799-805.
- [38] Zhang X, Wang Z, Xing H, Xiang Y, Lu Y. Catalytic and molecular beacons for amplified detection of metal ions and organic molecules with high sensitivity. Anal Chem. 2010;82:5005-11.
- [39] Wang Y, Nguyen K, Spitale RC, Chaput JC. A biologically stable DNAzyme that efficiently silences gene expression in cells. Nature Chem. 2021;13:319-26.
- [40] Zhang L, Kan A, Wang S, Xu X, Zhang N, Jiang W. DNAzyme walker induced DNAzyme working cascade signal amplification strategy for sensitive detection of protein. Sens Actuat B Chem. 2021;333:129551.
- [41] Zhou L, Xiong Y, Wang H, Yin A, Zhang X, Li H, et al. Targettriggered DNAzyme walker with 3D walking unit for copper species sensing in serum: a multivalent binding strategy for improving the detection performance. Sens Actuat B Chem. 2021;334:129589.
- Ma X, Ding W, Wang C, Wu H, Tian X, Lyu M, et al. DNAzyme [42] biosensors for the detection of pathogenic bacteria. Sens Actuat B Chem. 2021;331:129422.
- [43] Yang CJ, Cui L, Huang J, Yan L, Lin X, Wang C, et al. Linear molecular beacons for highly sensitive bioanalysis based on cyclic Exo III enzymatic amplification. Biosens Bioelectron. 2011;27:119-24.
- [44] Yang X, Tang Y, Mason SD, Chen J, Li F. Enzyme-powered threedimensional DNA nanomachine for DNA walking, payload release, and biosensing. ACS Nano. 2016;10:2324-30.
- [45] Huang J, Wu J, Li Z. Molecular beacon-based enzyme-free strategy for amplified DNA detection. Biosens Bioelectron. 2016;79:758-62.
- [46] Lou Y, Peng Y, Luo X, Yang Z, Wang R, Sun D, et al. A universal aptasensing platform based on cryonase-assisted signal amplification and graphene oxide induced quenching of the fluorescence of labeled nucleic acid probes: application to the detection of theophylline and ATP. Microchim Acta. 2019:186:494.
- [47] Fu H, Hu O, Fan Y, Hu Y, Huang J, Wang Z, et al. Rational design of an "on-off-on" fluorescent assay for chiral amino acids based on quantum dots and nanoporphyrin. Sens Actuat B Chem. 2019;287:1-8.
- [48] Jiang YS, Bhadra S, Li B, Ellington AD. Mismatches improve the performance of strand-displacement nucleic acid circuits. Angew Chem. 2014;126:1876-9.
- Zhu J, Ding Y, Liu X, Wang L, Jiang W. Toehold-mediated strand displacement reaction triggered isothermal DNA amplification for highly sensitive and selective fluorescent detection of single-base mutation. Biosens Bioelectron. 2014;59:276-81.
- Wang J, Chen S, Yuan R, Hu F. DNA branched junctions induced the enhanced fluorescence recovery of FAM-labeled probes on rGO for detecting Pb2. Anal Bioanal Chem. 2020;412:2455-63.
- [51] Song X, Wang Y, Liu S, Zhang X, Wang J, Wang H, et al. A triply amplified electrochemical lead(II) sensor by using a DNAzyme and via formation of a DNA-gold nanoparticle network induced by a catalytic hairpin assembly. Microchim Acta. 2019;186:1-8.

- [52] Yun W, Wu H, Liu X, Zhong H, Fu M, Yang L, et al. Ultra-sensitive fluorescent and colorimetric detection of UO22 based on dual enzyme-free amplification strategies. Sensors Actuat B Chem. 2018;255:1920-6.
- [53] Xiong E, Zhen D, Jiang L, Zhou X, Binding-induced, 3Dbipedal DNA. walker for cascade signal amplification detection of thrombin combined with catalytic hairpin assembly strategy. Anal Chem. 2019;91:15317-24.
- [54] Wang D, Guo R, Wei Y, Zhang Y, Zhao X, Xu Z. Sensitive multicolor visual detection of telomerase activity based on catalytic hairpin assembly and etching of Au nanorods. Biosen Bioelectron. 2018;122:247-53.
- [55] Yang L, Wu Q, Chen Y, Liu X, Wang F, Zhou X. Amplified microRNA detection and intracellular imaging based on an

- autonomous and catalytic assembly of DNAzyme. ACS Sens. 2018;4:110-7.
- [56] Yuan R, Yu X, Zhang Y, Xu L, Cheng W, Tu Z, et al. nanoassembly on quantum dots and DNAzyme-modulated double quenching for ultrasensitive microRNA biosensing. Biosens Bioelectron. 2017;92:342-8.
- [57] Luo J, Xu Y, Huang J, Zhang S, Xu Q, He J. Enzyme-free amplified detection of circulating microRNA by making use of DNA circuits, a DNAzyme, and a catalytic hairpin assembly. Microchim Acta. 2018;185:1-6.
- [58] Ren R, Bi Q, Yuan R, Xiang Y. An efficient, label-free and sensitive electrochemical microRNA sensor based on targetinitiated catalytic hairpin assembly of trivalent DNAzyme junctions. Sens Actuat B Chem. 2020;304:127068.